



On the Effect of Exposed Timber on the Severity of Structural Fires in a Compartment and Required Firefighting Resources

Shuna Ni *, Department of Civil and Environmental Engineering, Utah State University, 4110 Old Main Hill, Logan, UT 84322, USA

Thomas Gernay , Department of Civil and Systems Engineering, Johns Hopkins University, 3400 N Charles Street, Baltimore, MD 21218, USA

Received: 10 August 2021/**Accepted:** 11 April 2022/**Published online:** 23 May 2022

Abstract. Estimation of design fires and thermal exposure conditions is an important step in structural fire engineering procedures. Mass timber, as a combustible material, may contribute to the fire intensity, yet there lacks methods to estimate design fires in compartments with exposed timber. This paper summarizes available experimental data on the contribution of exposed timber to heat release rate, describes a simple analytical method to evaluate this contribution, and discusses the effects on time–temperature curves and required firefighting resources based on a case study. Results show that the total heat release rate in compartments increases with the surface of exposed timber. This total heat release rate can be conservatively estimated using empirical relationships for ventilation-controlled burning rate and charring depth. In estimating gas temperature–time curves, both external flaming and extended fire duration combustion models can be applied to obtain an envelope of fire severity inside the compartment and for external spread. The proposed assessment approach provides a method to evaluate realistic design fires in timber buildings and to estimate the water supply required to put out these fires. Accurate modeling of the contribution of timber to fire severity is important for the design of mass timber construction as well as for the safety of firefighters.

Keywords: Fire safety engineering, Mass timber, Cross-laminated timber, Heat release rate, Design fire, Firefighters

1. Introduction

The recent development of engineered wood products, including cross-laminated timber (CLT) panels and glulam framing members, has opened opportunities to build tall timber buildings, which attract increasing interest due to their environmental and aesthetic benefits. Completed projects include an 18-story student residence

*Correspondence should be addressed to: Shuna Ni, E-mail: shuna.ni@usu.edu



in Vancouver, a seven-story office tower in Minneapolis, the 18-story Mjøsa Tower in Norway, while many more are under consideration across the world. Due to the combustibility of timber, its use as a building material has traditionally been limited by restrictions in building regulations, but some jurisdictions are relaxing these restrictions to allow the use of mass timber for higher and larger buildings [1, 2].

All tall buildings pose specific challenges for fire safety. Evacuation and fire-fighting activities are complicated due to the building size, height, and/or occupancy. Therefore, egress strategy, firefighting operations, and consequences of failure for the building and the neighboring structures, need careful consideration. With mass timber construction, the fact that wood is a combustible material which may become involved in the fire needs to be accounted for when assessing the fire safety strategy. As empirical data on the fire behavior of tall mass timber buildings is missing, the successful implementation of mass timber in large urban constructions requires application of adequate fire safety engineering methods.

Current understanding of fire performance of timber structures is mostly restricted to standard time–temperature exposure, which is consistent with the approaches used for the majority of all buildings of all materials. Although the use of standard fires to determine fire resistance is the overwhelming majority of construction, it is insufficient to gauge the structure behavior under real fire conditions [2–7]. The design approach most commonly used in practice, based on standard fire resistance and sacrificial char layer, is not adequate to address the fire safe design of tall mass timber buildings, because it does not capture the possible contribution of timber to fuel the fire, disregards the vulnerability during the cooling phase, and fails to contemplate the issues of self-extinction and continued charring and smouldering. Herein, self-extinction refers to the intrinsic quality of timber when the flame heat flux is not sufficient to sustain its own flaming [8, 9]. Even in the case of self-extinction, glowing combustion and smouldering can occur. Researchers have raised concern that timber elements in tall wood buildings can increase the fire load, affect the fire growth rate, and potentially overwhelm fire protection systems in buildings, thereby generating more severe conditions for occupants and responding firefighters and increasing the threat of damage to adjacent properties [10]. Yet, data and methods are still lacking to address questions such as the ability of fire brigades to contain and extinguish a severe fire in a tall wood building and the risks associated with fire spread within the building and toward nearby structures.

In recent years, research on the fire performance of timber structures has intensified. In the US, a white paper was published by NIST in 2014 [3] to discuss a performance-based framework for the fire safety design of multi-story mass timber buildings. A multi-year project funded by the United States Forest Service on the “Fire Safety Challenges of Tall Wood Buildings” was carried on by the NRC Canada and RISE Sweden, and included CLT compartment fire tests conducted at the NIST [10] and engineering methods developed by RISE [11]. In Europe and Australia, experimental fire tests were conducted on CLT panels [12–15] and CLT compartments [16–19]. The Epernon fire test campaign improved understanding of the contribution of combustible construction material to the heat output in a standard fire resistance testing setup [13] and in large-scale compartment fire experiments [18]. Reduced-scale fire tests were conducted in Australia to explore the

factors that govern the fire behavior in mass timber open-plan compartments [17]. The behavior of timber under non-standard fire exposure has recently been studied by several research teams [20–25], including the issue of stability until full burnout [26]. Self-extinction of CLT and engineered wood products was also investigated [27–29], as well as specific issues such as glulam connectors [30–33]. Reflecting the broad and current interest, the fire safety challenges of tall timber buildings have been discussed in recent letters to the editor [34, 35] and professional publications [36].

Estimation of design fires and thermal exposure conditions in mass timber compartments is important to enable performance-based fire design. A better understanding of the impact of exposed timber on the fire development also informs the water supply and water flow requirements to support the safety of fire brigades. However, previous studies have highlighted the inadequacy of the conventional compartment fire framework in describing fire development in mass timber compartments [11, 37–42]. Researchers have used Fire Dynamics Simulator (FDS) to study the damage caused by fire in mass timber compartments [42], and improved its ability to model such fire by incorporating CLT pyrolysis models with charring criteria into it. Such expanded FDS fire-modeling techniques have been benchmarked against prior test results [43]. However, more efforts are needed to improve the accuracy of the simulation. Methods based on zone models have also been proposed to predict the heat release rate and gas temperature in a mass timber compartment [39–41]; and pragmatic design methods based on the parametric natural fire models were also proposed for predicting the evolution of gas temperature in a mass timber compartment [11, 37]. The method in [11] is iterative in nature and based on the parametric fire model in Eurocode [44], while the method in [37] was built on the parametric fire model developed by [45].

This paper describes an analytical method to evaluate heat release rate (HRR) in timber compartments, accounting for the contribution of exposed timber and compares the results with available experimental data. The model is based on the simplified combustion models of content fuel load in [46] and the wood charring model for parametric fire exposure in [47]. Based on the validated HRR model, a case study is conducted to investigate the impact of exposed timber surface on the severity of a mass timber compartment fire and its corresponding demand on firefighting sources. The fire safety design of a mass timber building includes layers of fire protection. However, quantifying the fire dynamics when other layers fail is crucial to assess the structural fire response, which has been indicated in the recent fire tests on large and open-plan compartments by a collaborative team of Imperial College, Arup, and CERIB [48]. Therefore, the case study in this paper will focus on the worst-case scenario where active fire safety measures fail.

2. Review of Existing Tall Mass Timber Buildings

Existing mass timber buildings in different countries were reviewed to evaluate the volume of timber used in these buildings. The volume of timber was obtained by reviewing documentation about the projects, such as press releases and technical

publications. Table 1 provides the ratio of the timber volume over the gross floor area. The gross floor area is defined as the sum of the building footprint of each story built in timber (i.e., for buildings with a concrete podium, the surface area of the concrete story is not counted). The ratio ranges between 0.14 and 0.64 m³/m², with mean of 0.31 m³/m² and coefficient of variation of 0.45.

The fuel load corresponding to the volume of timber used in existing mid- and high-rise timber buildings, listed in Table 1, is evaluated by considering the density and heat of combustion (i.e., calorific value) of the timber products. For CLT, the most commonly used species is spruce with a density from 480 kg/m³ to 500 kg/m³ [49]. Combining a timber density of 490 kg/m³ with the mean timber volume per square meter of 0.31 m³/m² yields a mean timber weight per square meter of 152 kg/m². The fuel load can then be estimated as $Q_{fi} = \sum M_i \cdot H_{c,net,i} \cdot \Psi_i$ (according to Eurocode [44]), with M_i the amount of combustible material in kg; $H_{c,net,i}$ the net calorific value (taken as 17.5 MJ/kg for wood) [21]; and Ψ_i the optional factor for assessing protected fire loads. The fuel load density is given by $q_f = Q_{fi}/A_f$, where A_f is the floor area of the fire compartment. The evaluation is made here for the highest bound, obtained with $\Psi_i = 1$ and no application of combustion factor. Therefore, the mean value of the fixed fuel load, resulting from the timber as a construction material, in the reviewed mass timber buildings is given by Equation 1:

$$q_{f, \text{tmb}} = 152 \text{ kg/m}^2 \times 17.5 \text{ MJ/kg} \times 1 = 2660 \text{ MJ/m}^2 \quad (1)$$

This estimation should not be taken as an exact estimate of the energy that would fuel a real fire in a completely engulfed mass timber building, but rather as an order of magnitude of the maximum available energy embedded in the structure. The actual contribution of the timber in a real fire would necessarily be less than this value due to the protection of gypsum boards, the existence of active fire-protection measures, and the fact that timber members would not be entirely consumed. However, if some of the timber from the structure are exposed and will become involved in a fire, it appears necessary to develop methods to account for this contribution in the fire safety engineering assessment.

3. Contribution of Exposed Timber to the HRR: Available Experimental Data

When timber elements are not shielded from the fire by insulative protection (e.g., encapsulation), these elements contribute to the fuel load, altering the fire dynamics by increasing the duration and intensity of the fire. This is particularly significant for lining elements with large surface area, such as CLT floors and walls. Several experimental studies have been conducted in the past decade on the fire dynamics in CLT compartments. The tests by Hevia [86], McGregor [43], and Su et al. [10] are further reviewed here to study the contribution of timber to the heat release during a fire.

Table 1
Amount of Timber in Existing Mid-Rise and High-Rise Mass Timber Buildings

Building	Year	Location	# stories	Gross floor area (m ²)	Volume of timber (m ³)	Timber volume/ area (m ³ /m ²)	Refs.
Brook common	2017	Canada	18 ^a	15,200	2233	0.16	[50]
T3	2016	USA	7 ^a	20,439	3600	0.21	[51, 52]
Stadthaus	2009	UK	9 ^a	2890	901	0.35	[53, 54]
Carbon12	2018	USA	8	3902	544	0.14	[55, 56]
Mjøstårnet	2019	Norway	18	11,300	2035	0.18	[57-59]
Origine	2017	Canada	13 ^a	13,124	3111	0.26	[60-62]
Banyan Wharf (The Cube)	2015	UK	10	6750	1313	0.19	[63-65]
Treet	2015	Norway	15 ^a	7140	935	0.14	[66]
Strandparken	2014	Sweden	8	15,924	4777	0.30	[67, 68]
Trafalgar Place	2015	UK	10	1800	820	0.46	[69, 70]
Via Cenni	2013	Italy	9	17,000	6100	0.36	[69, 71]
Lintuvuila	2013	Finland	6 ^a	3100	1300	0.50	[69]
Bridport House	2012	UK	8	4154	1576	0.38	[72, 73]
Forté	2013	Australia	10 ^a	1728	1000	0.64	[74]
Wood Innovation & Design Centre	2014	Canada	8	4820	1700	0.35	[75, 76]
25 King	2018	Australia	10 ^a	14,965	6239	0.46	[77-79]
Dalston Lane	2016	UK	10 ^a	15,960	4500	0.31	[80-82]
Holz8	2011	Germany	8	1740	570	0.33	[83]
HoHo	2019	Austria	24	25,000	4620	0.18	[84, 85]

^aFirst story is a concrete podium

Figure 1 shows the heat release rate (HRR) measured in the five tests by Hevia and McGregor [43, 86]. The tests were performed on an identical room, with varying degrees of protection for the timber members. The room was 4.5 m long by 3.5 m wide by 2.5 m high with a single opening of 1.07 m by 2 m. The average content fuel load from the furniture was 535 MJ/m². The degree of exposed (i.e., unprotected) surface of the timber members varied from 0% exposed (McGregor #2 and 4) to 100% exposed (McGregor #5) with intermediate values of 21% (Hevia #3, one wall exposed, 4.5 m by 2.5 m), 37% (Hevia #1, two adjacent walls exposed, 3.5 m by 2.5 m and 4.5 m by 2.5 m) and 42% (Hevia #2, two opposite walls exposed, 4.5 m by 2.5 m and 4.5 m by 2.5 m). The HRR was measured by the oxygen consumption calorimetry method, including the heat released both inside and outside the compartment. Figure 1 shows that as the exposed surface of CLT increased, the HRR increased. The test with 100% exposed timber surface yielded the highest HRR peak and overall heat released. Delamination occurred in all tests with 37% or more exposed surface, due to failure of the polyurethane-based adhesive when charring progressed to the interface layers, leading to re-ignition of the fire compartments (occurrence of second HRR peak in Hevia #1 and #2 and in McGregor #5). These tests were ended by the application of water. In contrast, the test with 21% exposed surface (Hevia #3) achieved self-extinction. In tests with 0% exposed surface (McGregor #2 and #4), the HRR curves continued to decay at a steady rate until the test ended.

Figure 2 shows the HRR measured in the six tests by Su et al. [10]. Six compartments of 9.1 m long by 4.6 m wide by 2.7 m high were tested. The inside of the compartments was fully or partially lined using multiple layers of 15.9 mm thick Type X gypsum board. Real residential contents and furnishings were used to provide a fuel load density of 550 MJ/m². Two baseline tests (Tests 1–1 and 1–2), with all CLT surfaces protected in the compartments (0% exposed) but of different ventilation configurations, defined the contribution of the moveable fuel load to the compartment fires and provided baseline data for quantifying the CLT contribution to the compartment fires in the other tests. Test 1–1 had an opening of 1.8 m wide by 2.0 m high while Test 1–2 has an opening of 3.6 m wide by 2.0 m high. The ventilation configuration of Test 1–3 is the same as that of Test 1–2 while the ventilation configuration of Tests 1–4, 1–5 and 1–6 is the same as that of Test 1–1. However, Test 1–3 has an exposed wall (W1, 9.1 m × 2.7 m, 23%); Test 1–4 has an exposed ceiling (9.1 m × 4.6 m, 37%); Test 1–5 has an exposed wall (W1, 9.1 m × 2.7 m, 22%); Test 1–6 has a combination of exposed ceiling (9.1 m × 4.6 m) and wall (W1, 9.1 m × 2.7 m); the total percentage of exposed timber surface for Test 1–6 is 59%. In the tests, the exposed CLT surfaces exhibited heat delamination, which led to one or more periods of significant fire regrowth after decay in three of the tests, and no decay of the fire prior to suppression in the sixth test. The ventilation conditions had significant impact on the fire development in the compartments, as well as on the CLT contribution to the fire.

The total heat release in the tests of Figures 1 and 2 have been calculated over a reference duration and plotted in Figure 3. For Figure 1, the total heat release is evaluated over the first 26 min. For Figure 2, it is evaluated over the first

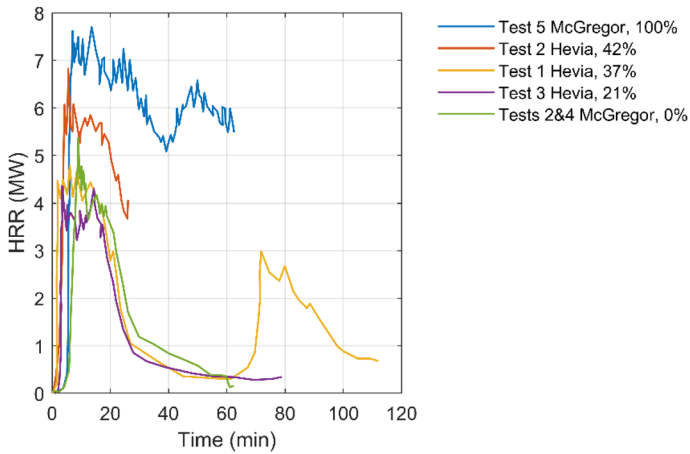


Figure 1. HRR in the fire compartment tests by McGregor [86] and Hevia et al. [43]. The percentage indicates the relative surface of timber exposed.

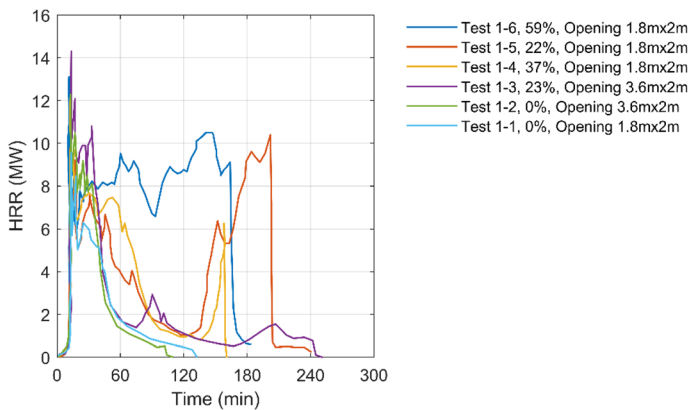


Figure 2. HRR in the fire compartment tested by Su et al. (2018) [10]. The percentage indicates the relative surface of timber exposed.

110 min. These totals are normalized by the total heat release in the case of the reference test with 0% of the timber surface exposed. The heat release from Hevia's Tests 1, 2 and 3 and McGregor's Test 5 are normalized by the average of McGregor's Tests 2 and 4. The heat release from Su's Tests 1–4, 1–5 and 1–6 are normalized by that of the Test 1–1; while the heat release from Su's Test 1–3 is normalized by that of Test 1–2. Figure 3 shows that as the area of the exposed timber surface increases, the total heat release increases with almost linear trend. However, the slope varies between the different test sets, indicating a dependence

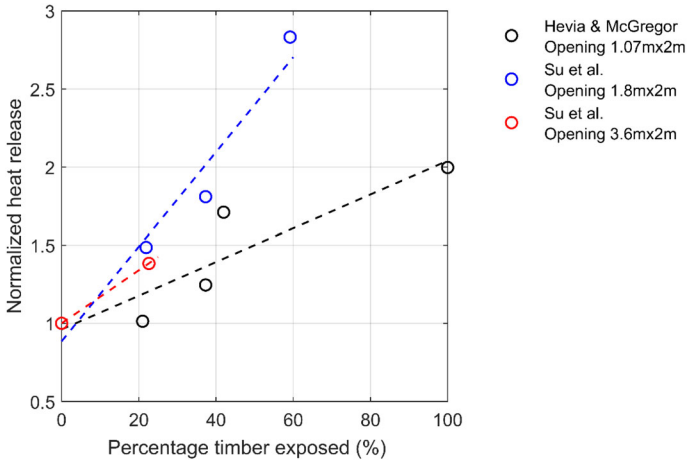


Figure 3. Effect of exposed timber surface on the total heat release (over a reference duration) during fire tests on mass timber compartments.

on factors such as the dimensions and ventilation conditions of a fire compartment, and the movable fuel load.

The test data was further analyzed to derive the HRR contributed by square meter of exposed CLT. The HRR attributable to the CLT for the tests discussed above is obtained by taking the difference between the total HRR of the considered test and that of the corresponding baseline test in which the timber was fully protected (0% exposed). As the area of exposed timber surface increases, the contribution of CLT to the total HRR increases. This contribution can reach 7 MW in the first set of tests and 10 MW in the second. Then, the HRR contributed by timber per square meter of exposed CLT is obtained by dividing the HRR con-

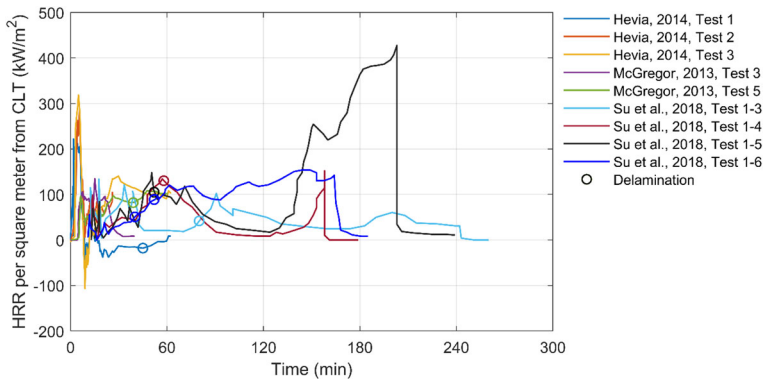


Figure 4. Timber contribution to HRR per exposed surface of CLT panels, from tests [10, 43, 86].

tributed by the CLT by the surface area of the exposed timber (A_{imb}). It is noted $\dot{q}_{f,imb}$ and is plotted in Figure 4. In Figure 4, the circles on the plots indicate the start of delamination. The HRR attributable to the exposed timber mostly ranges between 0 kW/m² and 100 kW/m² of exposed CLT panel. Extreme values of 300 kW/m² and -100 kW/m² are observed temporarily. The temporary occurrence of negative values is likely due to the adopted method to evaluate CLT contribution by difference of two tests rather than by direct measure, with the uncertainties and approximations that this entails. It is also noted that volatiles contributed by CLT may be transported away and not combusted [43]. In most tests, as the delamination of CLT begins, the $\dot{q}_{f,imb}$ will regrow, as shown in Figure 4. In the calculation of $\dot{q}_{f,imb}$, the initial value of the exposed timber surface is used, which may lead to large values at the later stage of some tests when additional timber surfaces get involved due to failure of fire protection, which significantly increases the HRR (such as the Test 1-5 by Su in which, during the last 10 min, all walls and ceiling surfaces were burning). Based on Figure 4, a conservative estimate of the HRR per square meter of exposed CLT, sustained over a reasonable duration, is: $\dot{q}_{f,imb} = Q_{imb}/A_{imb} = 100 \text{ kW/m}^2$.

4. Contribution of Exposed Timber to the HRR: Simple Evaluation Method

4.1. Description of the Method

As discussed in Sect. 3, the additional heat release rate (HRR) contributed by exposed timber can be measured from tests. The HRR contributed by square meter of exposed timber can also be evaluated analytically. The fire dynamics of timber compartments is a very complex issue that is still the focus of much research efforts [15, 48, 87-90]. In this section, simplifying assumptions are adopted to allow a reasonable analytical evaluation of the heat output from burning timber in mass timber buildings; while the empirical data of Sect. 3 serves as a benchmark. The following simple evaluation method is only suitable where a CLT panel has bond line integrity and encapsulation is in place for the full duration of a fire.

In fuel-controlled conditions, the EN 1991-1-2 [44] evaluates the maximum HRR associated to the movable content fuel in different occupancies as $A_f \cdot RHR_f$, where A_f is the floor area of a fire compartment and RHR_f is the maximum heat release rate density of movable content fuel loads (given in Table E.5. of the EN 1991-1-2 [44]).

However, for ventilation-controlled conditions, the combustion is limited by the availability of oxygen, and the maximum HRR inside the compartment (Q_{vent}) is estimated by Equation 2:

$$Q_{vent} = H_{c,eff} \cdot \dot{m} \quad (2)$$

where $H_{c,eff}$ is the effective heat of combustion of fuel (MJ/kg) and \dot{m} is the burning rate (kg/s). The effective heat of combustion is given by: $H_{c,eff} = m \cdot H_{c,net}$, where $H_{c,net}$ is the net calorific value (17.5 MJ/kg for wood) and m is the combustion factor (0.8). An empirical relationship for the ventilation controlled burning rate is given by Equation 3 [91]:

$$\dot{m} = k_p \cdot A_v \cdot \sqrt{h} \quad (3)$$

where A_v is the total area of wall openings (m^2); h is the weighted average height of openings (m); and k_p is the combustion factor (pyrolysis coefficient) which can be estimated by Equations 4 and 5:

$$k_p = \frac{1}{148 \cdot F_{O_2} + 3.8} \quad (4)$$

$$F_{O_2} = A_v \cdot \sqrt{h} / A_{T2} \quad (5)$$

where A_{T2} is the total internal surface not including openings. The relationships of Equations 4 and 5 are equivalent to EN1991-1-2 (E.6) when the factor k_p is approximated as 0.10.

In ventilation-controlled conditions, the products of pyrolysis cannot be entirely consumed in the compartment at the time they are released due to lack of oxygen. Two models are typically adopted in structural fire engineering to account for the energy contained in the unburned pyrolysis products: an external flaming combustion model and an extended fire duration combustion model. The external flaming combustion model assumes that there is external burning, meaning that the total pyrolysis rate of a compartment fire remains unchanged but the extra pyrolyzed fuel burns outside (Figure 5a). The extended fire duration combustion model

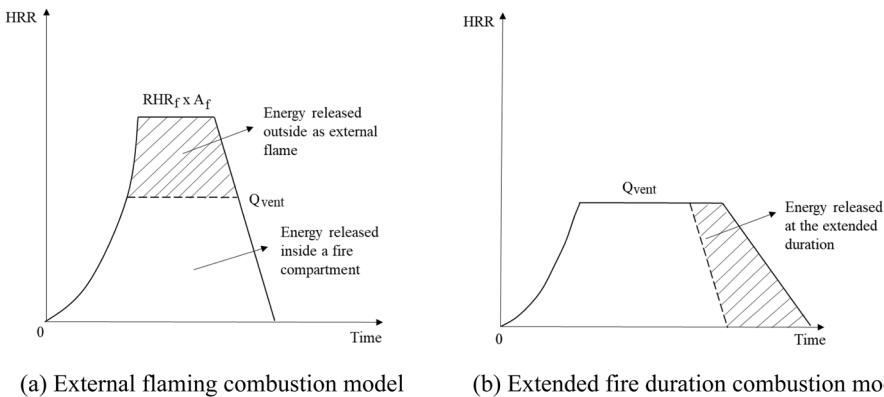


Figure 5. Combustion models for ventilation-controlled compartment fires [46].

tion model supposes that the total mass of fuel is burnt inside the compartment under the ventilation-controlled maximum heat release rate Q_{vent} , meaning that the curve of the HRR is extended to correspond to the available energy given by the fire load (Figure 5b). This is the most conservative assumption from the standpoint of the maximum amount of energy inside the compartment. Observations from compartment fire experiments with exposed timber show that the contribution of timber results in both increased heat released outside and increased burning duration inside the compartment [13].

For ventilation-controlled compartments with exposed timber, the two models of Figure 5 can be adapted to account for the heat output from the timber surfaces. In theory, the maximum possible HRR is equal to the sum of that of the content fuel plus that of the exposed timber as given by Equation 6:

$$Q_{max} = A_f \cdot RHR_f + Q_{tmb} \tag{6}$$

The maximum HRR inside the compartment is limited by Equation 2, while the excess HRR can be released outside (Figure 5a) or can extend the fire duration (Figure 5b). Figure 6 presents the HRR in ventilation-controlled compartments with exposed timber. The envelope HRR curve in Figure 6a shows the maximum possible HRR (assuming that timber charring begins when the fire comes to flash-over). The red curves represent the HRR inside the compartment. In the external flaming model (Figure 6a), the maximum HRR, Q_{max} , is reached but part of it is released outside the compartment. The blue area is the energy contributed by the movable content fuel, equal to $q_{f,mc} \cdot A_f$. The yellow area is the energy contributed by the exposed timber surface, equal to $q_{f,tmb} \cdot A_{tmb}$. Here, $q_{f,mc}$ is the effective fire load density from movable contents relative to floor area (A_f), while $q_{f,tmb}$ is the effective fire load density from the exposed timber surface relative to the area of exposed timber surfaces (A_{tmb}).

The HRR and fuel load contributed by the exposed timber surface can be evaluated from wood charring models. The charring depth is evaluated as a function

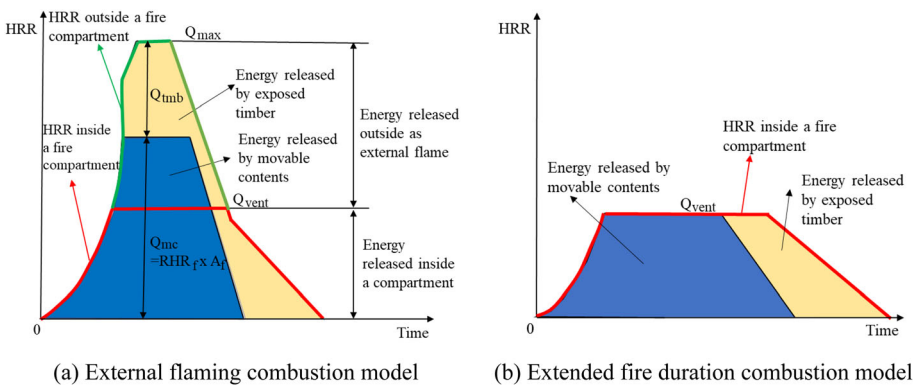


Figure 6. Combustion models for ventilation-controlled fires in CLT compartments.

of time according to the model in Eurocode 5 part 1–2, Annex A for parametric fire exposure [47]:

$$d_{char,t} = \beta_{par} \cdot t \quad t \leq t_o \quad (7)$$

$$d_{char,t} = \beta_{par} \cdot \left(1.5t - \frac{t^2}{4t_o} - \frac{t_o}{4} \right) \quad t_o < t \leq 3t_o \quad (8)$$

$$d_{char,t} = 2 \cdot \beta_{par} \cdot t_o \quad t \geq 3t_o \quad (9)$$

β_{par} is the initial charring rate, calculated according to Equation 10:

$$\beta_{par} = 1.5 \cdot \beta_o \cdot \frac{0.2\sqrt{\Gamma} - 0.04}{0.16\sqrt{\Gamma} + 0.08} \quad (10)$$

where β_o is the one-dimensional charring rate corresponding to standard fire resistance tests following ISO 835. The one-dimensional charring rate corresponding to softwood is 0.65 mm/min according to most design standards [11]. Γ is the heat rate/time factor, the calculation of which refers to the parametric fire model in the Eurocodes [44]. The time period with a constant charring rate, t_o , is calculated in minutes as $t_o = 0.009 \cdot q_t / O$, where O is the opening factor, the calculation of which refers to the parametric fire model in the Eurocode [44]. q_t is the effective fire load density relative to the total surface area of the enclosure A_{T1} (including openings) (note: it is different from q_f).

The final thickness of the char layer, given by Equation 9, is reached when the time reaches $3t_o$; it is noted $d_{char,3t_o}$. The final total fuel load density contributed by the exposed timber surface, relative to the exposed timber surface, is estimated by Equation 11. Equation 11 is only applicable where a CLT panel has bond line integrity for the full duration of a fire.

$$q_{f,tmb}(3t_o) = \int_0^{d_{char,3t_o}} a_1 dd_{char} \quad (11)$$

where a_1 is the heat release per square meter per mm of charring depth.

The HRR per square meter contributed by the exposed timber, $\dot{q}_{f,tmb}(t)$, at any time is then obtained by time derivation of Equation 11, where $d_{char,3t_o}$ is replaced by the charring depth of timber at any time, $d_{char,t}$:

$$\dot{q}_{f,tmb}(t) = \frac{dq_{f,tmb}(t)}{dt} \quad (12)$$

The maximum HRR corresponding to the exposed timber, Q_{tmb} , is then evaluated as:

$$\dot{q}_{f,tmb,max} = \max(\dot{q}_{f,tmb}) \quad (13)$$

$$Q_{tmb} = A_{tmb} \cdot \dot{q}_{f,tmb,max} \quad (14)$$

4.2. Validation of the Method

The analytical method has been applied to predict the total HRR in the eleven compartments tests by Hevia, McGregor and Su et al. In the tests by Hevia and McGregor, the ratio of exposed surface to the total surface of the timber CLT panels was 100% (Test 5 by McGregor), 42% (Test 2 by Hevia), 37% (Test 1 by Hevia), 21% (Test 3 by Hevia), and 0% (Tests 2&4 by McGregor). All of those tests by Hevia and McGregor have the same compartment size (4.5 m long by 3.5 wide by 2.7 m high) and opening size (1.07 m by 2 m) (Noted as Group 1). These tests by Su et al. have the same compartment size (9.1 m long by 4.6 m wide by 2.7 m high) but have different opening sizes: Test 1–1 (0%), Test 1–4 (37%), Test 1–5 (22%) and Test 1–6 (59%) have an opening size of 1.8 m by 2 m (Noted as Group 2) while Test 1–2 (0%) and Test 1–3 (23%) have an opening size of 3.6 m by 2 m (Noted as Group 3). The method is applied with the external burning model assumption (Figure 6a).

The EN 1992-1-1 provides fire growth ratse ('slow', 'medium' and 'fast') and maximum heat release rates produced by unit area of fire (RHR_f) for different occupancies. In real scenarios, these two parameters vary, depending on many factors, e.g., fuel types. In this section, we use the baseline tests with 0% exposed timber surface to calibrate those two parameters, and then use the same calibrated parameters for all others tests in each group. The calibrated tests are shown in Figures 9(d), 10(a) and 11(a). The calibrated fire growth rate is "fast", "medium", "medium" for Group 1, Group 2, and Group 3, respectively. The corresponding time to reach a heat release rate of 1 MW is 150 s for "fast" and 300 s for "medium". The calibrated RHR_f is 250 kW/m², 150 kW/m² and 200 kW/m² for Group 1, Group 2 and Group 3, respectively. Here, it is assumed the combustion factor for the movable fuel load is 0.8.

Based on the calibrated parameters for the fire growth rate and RHR_f , further calibration on the burning of exposed timber surfaces is conducted. Figure 7 compares the experimental and predicted evolution of charring in the tests by Hevia and McGregor. The dash lines in Figure 7 are the measured evolution of charring in the exposed timber surfaces while the solid lines are the values predicted with Equations 7–9. For Test 1 by Hevia, the analytical model can well predict its initial charring evolution. However, the measured charring rate decreases significantly at 20 min, which cannot be captured by the analytical model. For Test 2 and Test 3 by Hevia and Test 5 by McGregor, Equations 7–9 can reasonably predict the measured charring. Therefore, no calibration is conducted on the parameters in these equations. In Equation 11, the parameter a_1 is defined as the heat release per square meter per mm of charring depth. a_1 is assumed to be 2.7 MJ/m²mm at the beginning and then linearly increase to 5.39 MJ/m²mm until the

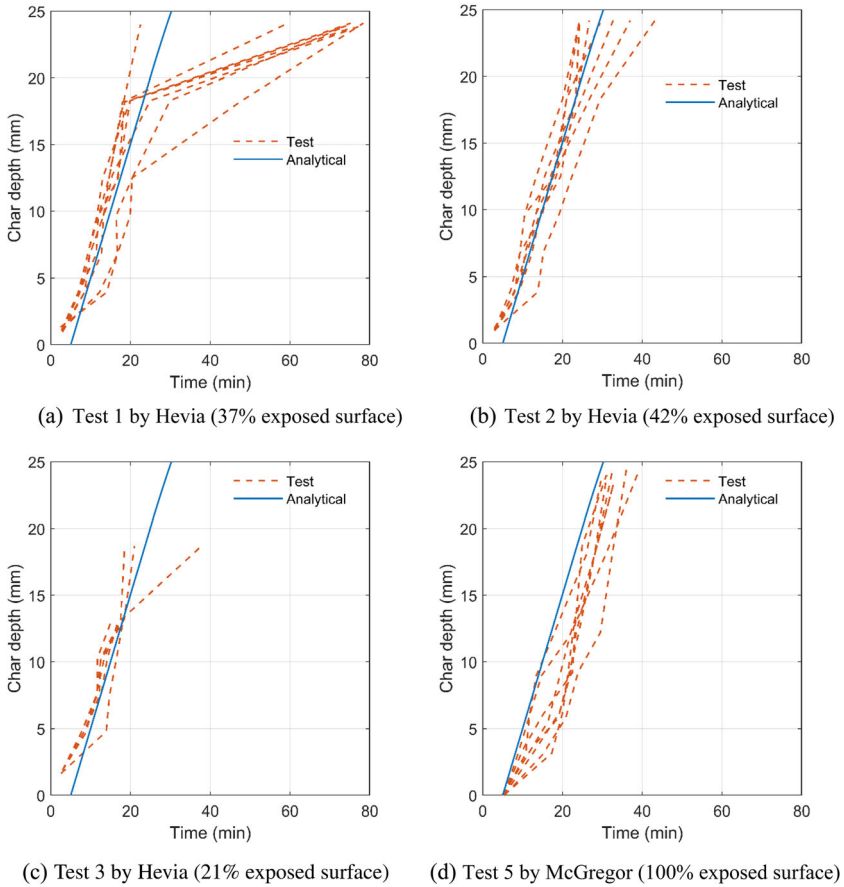


Figure 7. Comparison between measurements and analytical predictions for char depth.

charring depth is 10 mm in [39], as shown in the blue line in Figure 8. In real scenarios, this parameter is a function of many factors, such as the external heat flux, the gas velocities and the degree of turbulence at exposed surfaces [92]. Sensitivity studies shows that 70% of the proposed a_1 shown in Figure 8 (orange line) can reasonably predict the contribution of exposed CLT to the final HRR curve in most tests.

Figures 9, 10 and 11 compare the experimental (orange dash lines) and analytical (blue solid lines) HRR curves. For tests where delamination occurred, the time of first observation of delamination is marked by a circle on the plot. The proposed analytical method for prediction of HRR with contribution from timber only applies up to occurrence of delamination. The figures show that the analytical method can capture the increase in HRR resulting from an increase in exposed surface. For most tests by Hevia and McGregor, the initial increase rate of the HRR is accurately predicted. In the tests by Su et al., the experimental HRR

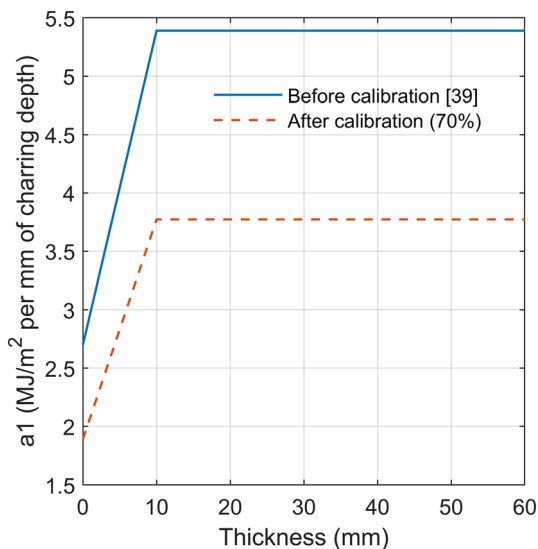


Figure 8. Heat released per square meter per mm of charring depth.

increases relatively slowly at the very beginning of the ascending branch, which cannot be captured by the analytical method. However, the analytical method can catch up to the experimental results around 10 min. The peak value of the HRR curves is reasonably predicted for most tests, especially for Test 5 by McGregor and Tests 1–3 and 1–5 by Su et al. Besides, the analytical method reasonably predicts the descending branch of the HRR curves before the delamination of CLT panels begin, especially for Test 2 by Hevia and Tests 1–3 and 1–5 by Su et al.

The experimental studies by McGregor have also calculated the total energy contributed by the movable fuel load is 366 MJ/m^2 , which is much lower than the value estimated by the content, $535 \times 0.8 \text{ MJ/m}^2$ (estimated average movable fuel load of the five tests by Hevia and McGregor multiplied by a combustion factor 0.8). If 366 MJ/m^2 is used as the efficient movable fuel load to calculate the HRR curves for the tests by Hevia and McGregor, the analytical results are closer to test results, compared to the results based on the estimated efficient movable fuel load (as shown in the dash blue lines labelled “Analytical*” in Figure 9).

5. Evaluation of Required Firefighting Resources

In the previous section, a method was provided to quantify the additional heat contributed by exposed timber in a fire. Part of this heat will remain in the compartment increasing the severity of the thermal exposure conditions for the structure, while part of it will be released outside the building which may put neighboring structures at greater risk of ignition. In both cases, this contributed heat has implications for fire brigades. In firefighting, enough water should be supplied to absorb the heat generated from a fire at a rate that can control and

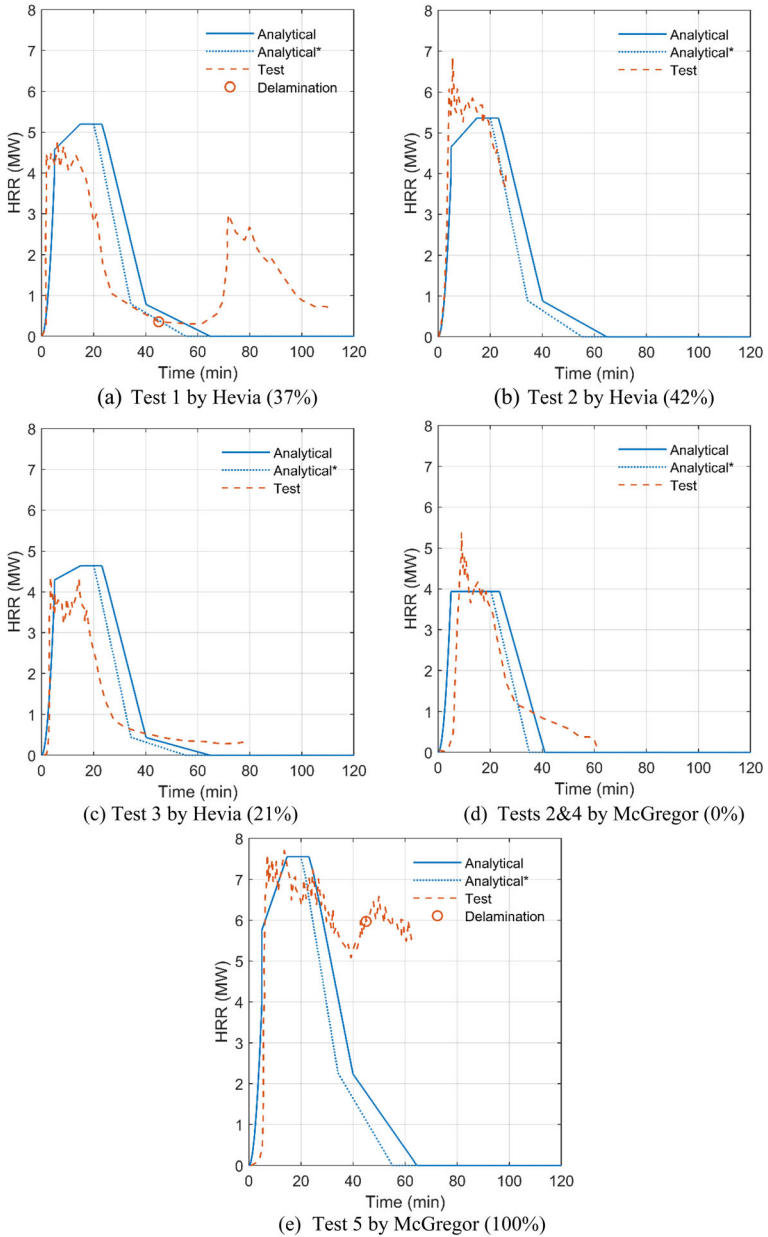


Figure 9. Comparison between the measured HRR in the compartment tests by Hevia and McGregor and the predictions using the analytical method (opening size: 1.07 m × 2 m).

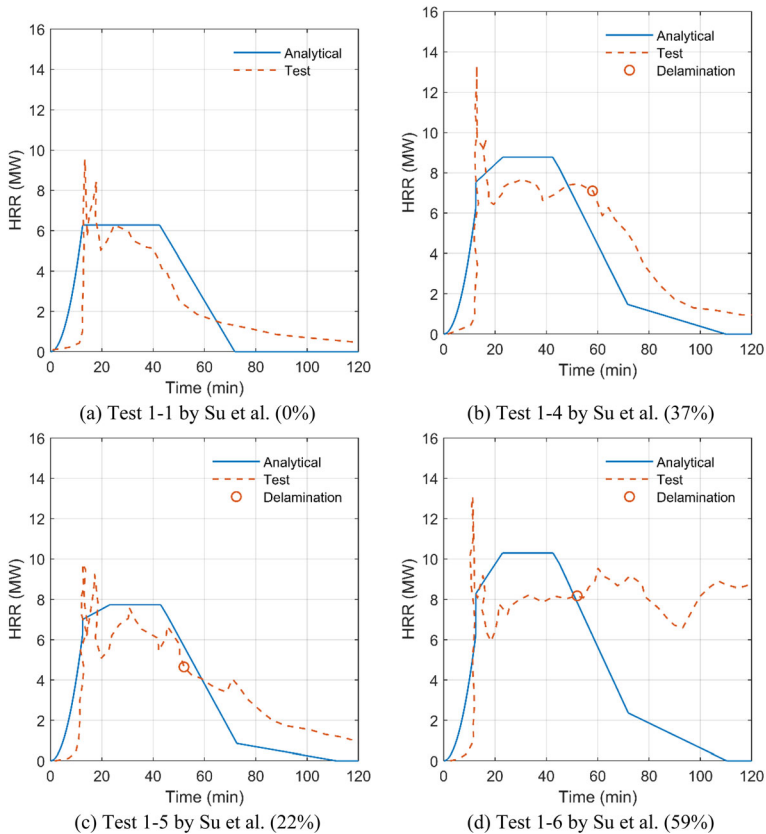


Figure 10. Comparison between the measured HRR in the compartment tests by Su et al. and the predictions using the analytical method (opening size: 1.8 m × 2 m).

finally extinguish a fire effectively. This consideration governs the requirements for fire flow (in L/s) and total water supply (in L) to fight a fire. The evaluation of the required quantity of water to effectively control the fire is a primary consideration for firefighters, with consequences on needed resources and implementation of tactical operations. This evaluation relies on a balance between the heat-absorbing capacity of water and the heat generated by the fire.

Most existing methodologies for evaluating fire flow and water supply are empirical or physical-empirical methods. Those methodologies consider the impact of building geometries (including volume, floor area, height, or non-divided developed surface area of a building). The method proposed by Iowa State University only considers the geometry of a building. The ISO method [93], NFPA 1142 method [94], Ontario Building Code method [95] and UK National Guidance Document on the Provision of Water for Firefighting method [96] consider more variables, such as construction materials, surrounding environments (distance between buildings, properties of exposure building, hazard exposure, communica-

tions between buildings, etc.) and fire-safety measures (e.g., whether a building is sprinklered), in addition to occupancy type and dimensions of a building. The International Fire Code (IFC) and NFPA 1 methods [97, 98] are tabulated values, based on a simplified ISO method. Yet, the methods discussed above do not allow evaluating the specific influence of the contribution of exposed timber on the water requirements.

A physics-based method is proposed in the New Zealand SFPE Method TP 2004/1 [99]. This method is used in this study to evaluate the impact of exposed timber on firefighting water requirements. According to this method, the required fire flow, F in L/s, to fight a fire is given by Equation 15. The equation numerator is the effective heat from a fire that is retained in the compartment, where Q_{\max} is the maximum heat release rate of the fire (MW), and k_F is a heating efficiency factor which can conservatively be estimated as 0.5 [99]. The equation denominator is the effective heat-absorbing capacity of water per unit volume. Q_w is the absorptive capacity of water at 100°C (MJ/L), including the energy to heat water from ambient temperature to the boiling temperature of 100°C and the energy to convert water to steam. Water has a specific heat capacity in liquid form of 4.18 kJ/kgK and a heat of vaporization of 2.26 MJ/kg, resulting in Q_w equal to 2.6 MJ/L. The factor k_w is the heat-absorbing efficiency of water, which is conservatively estimated as 0.5 [99]. The latter accounts for losses when applying water from a fire main to fight a fire.

$$F = \frac{k_F \cdot Q_{\max}}{k_w \cdot Q_w} \quad (15)$$

The New Zealand SFPE Method TP 2004/1 does not specify how to calculate Q_{\max} . Adopting the external flaming combustion model (Figure 6a), the maximum HRR, Q_{\max} , can be calculated using Equation 6. This value of Q_{\max} for the fire flow estimation is conservative, as it includes the heat released both inside and outside the compartment. While heat released outside should not be included when assessing the temperatures in the fire compartment, this heat may be relevant to the firefighting efforts and affect the amount of water needed to fight the fire. Indeed, fire accidents in tall buildings have shown the importance of actively controlling the spread of external flame along the façade. Meanwhile, if the fire is fought from outside, the heat from the external flames will need to be taken into account in the energy balance against water. Finally, the accurate assessment of the HRR inside a timber compartment depends on the complex interaction of many variables such as the ventilation conditions and geometry of the room, which will vary from case to case, hence it is reasonable to adopt an upper bound estimation. Therefore, it is chosen to conservatively adopt Q_{\max} from Equation 6 in the evaluation of the fire flow from Equation 15. This yields Equation 16 for the evaluation of the upper-bound fire flow in fire compartments constructed from mass timber:

$$F_{upper} = \frac{k_F(Q_{mc} + Q_{tmb})}{k_w \cdot Q_w} \quad (16)$$

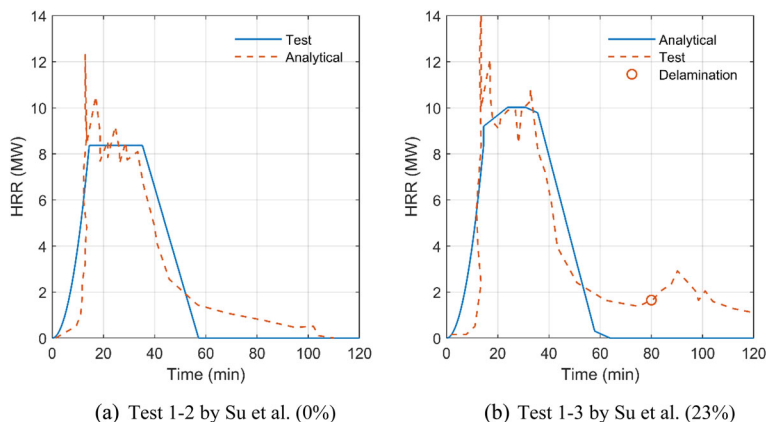


Figure 11. Comparison between the measured HRR in the compartment tests by Su et al. and the predictions using the analytical method (opening size: 3.6 m × 2 m).

where Q_{mc} is the maximum HRR associated to the movable content fuel in different occupancies, equal to $A_f \cdot RHR_f$ (referring to Table E.5 in the EN 1991–1-2 [44]); and Q_{tmb} is the maximum HRR associated to the exposed timber, estimated by Equation 14.

Adopting a similar reasoning, a method is provided in the New Zealand SFPE Method TP 2005/2 [100] for the total water supply. The total water supply (in L) can be approximated by expressing the balance between the total (effective) heating potential of the fuel load in a compartment and the (effective) heat-absorbing capacity of the water for unit volume. This yields:

$$S = \frac{k_F \cdot E}{k_w \cdot Q_w} SM \quad (17)$$

where E is the total (effective) fuel load (MJ) (with a combustion factor of 0.8), and SM is a safety coefficient recommended as 1.3 [100]. The upper-bound total water supply is thus estimated by Equation 18, where the energy E accounts for the contribution of the effective exposed CLT surfaces (yellow area in Figure 6) plus the effective movable fuel load in a compartment (blue area in Figure 6):

$$S_{upper} = \frac{k_F \cdot [q_{f,mc} \cdot A_f + q_{f,tmb}(3t_o) \cdot A_{tmb}]}{k_w \cdot Q_w} SM \quad (18)$$

where $q_{f,mc}$ is the effective movable (content) fuel load per square meter of floor area accounting for the combustion factor (m), 0.8, as recommended by Eurocode [101]; and $q_{f,tmb}(3t_o)$ is the effective fuel load per square meter of exposed timber surface, contributed by the exposed timber surface, estimated by Equation 11.

It is worth mentioning that if it is a high-rise fire, external firefighting is normally not carried out as the height is beyond the capability of firefighting equipment. If firefighting only occurs internally, Q_{\max} in Equation 15 is replaced by the maximum heat release rate in a compartment and E in Equation 17 is replaced by the energy that burns internally.

6. Case Study

A 10-story mass timber residential building is considered as a case study. The floor plan of the building is shown in Figure 12. The story height is 3 m. The fire is assumed to occur in compartment C1 at the second story. The ratio of opening area to the total enclosure surface of C1 (opening ratio A_v/A_{T1}) is 0.03, with opening height of 1.5 m; here A_{T1} is the total area of the enclosure surface of a compartment, including the floor area and the opening area. The enclosure thermal insulation parameter b is $770 \text{ J/m}^2\text{s}^{1/2} \text{ K}$ [11]. The movable fuel load density is 550 MJ/m^2 (movable fire load density used in most previous mass timber compartment fire tests [10, 43, 86]), and the effective movable fire density ($q_{f,m}$) is $0.8 \times 550 = 440 \text{ MJ/m}^2$. It is assumed that the fire growth rate is “medium” and RHR_f for movable fuel load is 250 kW/m^2 . The density of timber (ρ) is 490 kg/m^3 and its net heat of combustion ($H_{c,\text{net}}$) is 17.5 MJ/kg . The effect of sprinkler systems is neglected, as the case study focuses on the worst-case situation to quantify the fire dynamics when active fire-safety measures fail. This is crucial for assessing the structural fire response as a necessary layer of the fire safety strategy for those

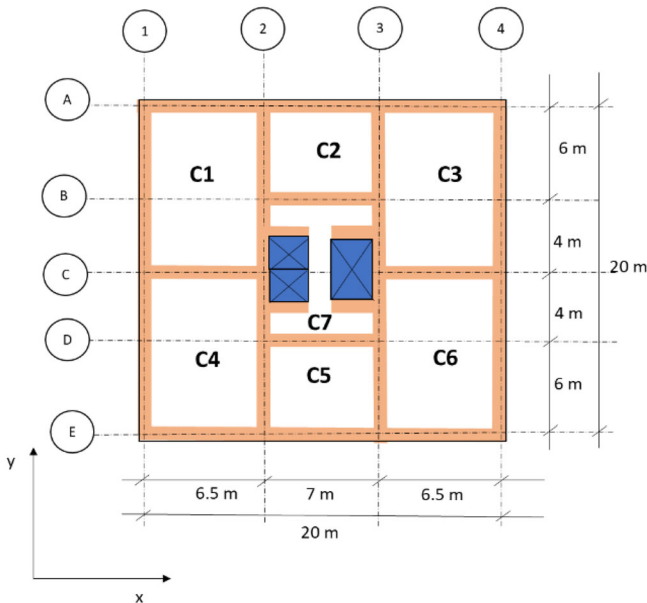


Figure 12. Floor plan of the building.

scenarios where fires grow uncontrolled due to the failure of active fire-protection measures. No active fire-protection measure has 100% efficiency. Such worst-case scenarios also exist in some extreme events, e.g., post-earthquake fire. Earthquakes can damage both passive (e.g., gypsum boards) and active fire safety measures (e.g., sprinkler system) and meanwhile cause dozens of building fires in a community [102].

6.1. HRR

Five different percentages of exposed timber are considered, 0% (fully protected), 25%, 50%, 75% and 100% (fully exposed), relative to A_{T2} . Here A_{T2} is the total area of the enclosure surface of the compartment C1 minus the floor area and the opening area. The HRR calculation is conducted using both the external flaming combustion model and the extended fire duration combustion model, to capture the boundaries of the expected behavior. This results in a total of 10 configurations. It is assumed that the fire remains contained in the compartment of origin and that CLT panels have bond line integrity and encapsulation is in place for the full duration of a fire.

Results of the HRR calculations are plotted in Figure 13. The HRR inside the compartment is bounded by Q_{vent} (Equation 2). In a ventilation-controlled fire, the energy from the timber is either released outside (external flaming), or remains in the room and extends the duration of the fire (extended duration); or a combination of both. The total fuel load contributed by the exposed timber is represented by the yellow area. The final charring depth of timber (d_{char}) is calculated according to Equation 9 and then the fuel load per square meter of exposed timber surface $q_{f,tmb}$ is calculated according to Equation 11. As the percentage of exposed timber surface increases from 0 to 100%, the peak HRR calculated based on the external flaming combustion model increases from 16.25 MW to 23.82 MW, which is relatively high compared to the results from small mass timber compartment fire tests but is close to those from medium mass timber compartment fire tests. For example, in the tests by Zelinka et al. ($A_f = 84 \text{ m}^2$) [103], the peak HRR value is close to 25 MW.

For the case with 50% of CLT exposed, the calculated HRR per square meter of exposed CLT, $\dot{q}_{f,tmb,max}$, is equal to 0.048 MW/m^2 . The final charring depth is equal to 46.9 mm. As a result, the effective fuel load contributed by the exposed CLT is 167 MJ/m^2 of exposed surface (202 MJ/m^2 relative to the floor area) for the compartment C1.

6.2. Time–Temperature Curves

The effect of the contribution of exposed timber on the gas temperature in the compartment was evaluated next. Gas temperatures in the compartment were evaluated using the zone model software OZone developed at Liege University [104]. The HRR from Figure 13 were used as input in the calculation. The results for the evolution of the gas temperature are shown in Figure 14. Ten curves are plotted corresponding to the ten configurations, i.e., five ratios of exposed timber and either the external flaming combustion or extended fire duration combustion model.

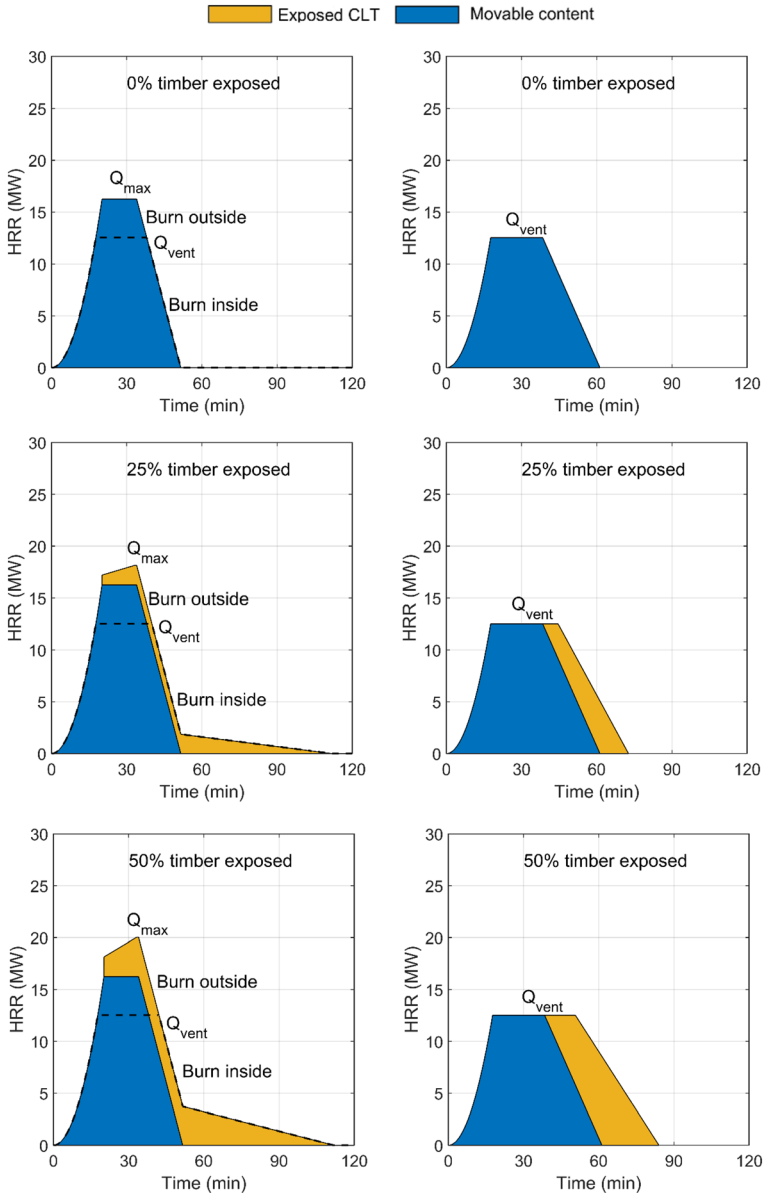


Figure 13. HRR for a fire in compartment C1 for different amount of exposed surfaces of timber lining, assuming that CLT panels have bond line integrity for the full duration of a fire.

The initial phase of the fire does not depend on the contribution of exposed timber. The temperature rises steadily for about 32 min until reaching a peak of about 1200°C. Thereafter, the gas temperature rises at a slower rate until eventu-

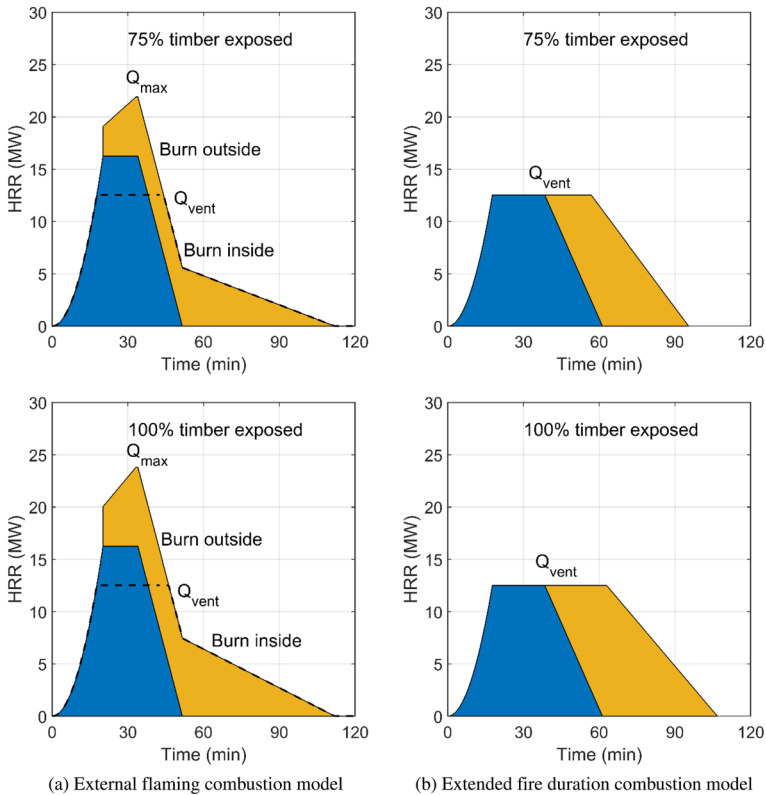


Figure 13. continued.

ally reaching a cooling phase. However, the duration of the fully developed phase of the fire increases significantly with increasing ratios of exposed timber. With the external flaming combustion model, the duration of the maximum temperature phase increases from about 39 min to 47 min when the ratio of exposed timber changes from 0% to 100%.

For the scenario with all the CLT panels protected, the temperature curve based on the extended fire duration combustion model is only slightly extended compared to that based on the external flaming combustion model. As the percentage of timber surface increases, the heating phase of the temperature curves based on the extended fire duration combustion model becomes significantly longer than that from the external flaming combustion model. This is because, with the exposed timber, there are more combustible gases released in the compartment that cannot react immediately with the oxygen, but burn later once the content fuel load is burned out. The maximum compartment temperature based on the extended fire duration combustion model is also greater than that based on the external flaming combustion model. Therefore, the assumption regarding the location of consumption of the products of pyrolysis in the oxygen-deprived compartment has important impact on the fire severity in the compartment. The real-

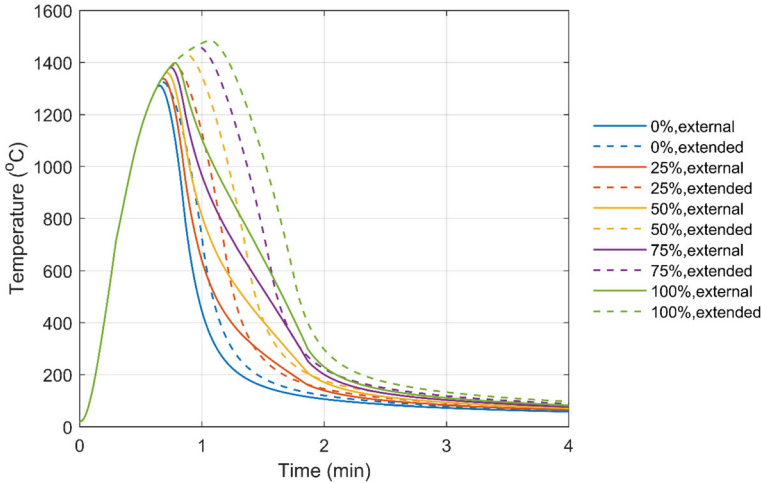


Figure 14. Compartment temperature curves for different amount of exposed surfaces of timber lining (Movable fuel load density is 550 MJ/m^2).

ity likely lies in between the boundary cases of external flaming and extended duration [13]. Overall, the durations of the heating phase of the curves range from 39 min to 64 min.

The temperature curves in Figure 14 are based on the assumption that the movable fuel load is 550 MJ/m^2 , which is lower than the average fuel load density for dwelling recommended by Eurocode [44]. If the movable fuel load is equal to the average fuel load density for dwelling, 780 MJ/m^2 , the compartment temperature curves are shown in Figure 15. All the peak temperatures are greater than 1400°C , which are not very significantly different from the peak values in Figure 14. However, the fire duration increases with the increase in content fuel load, ranging from 49 min to 86 min.

The peak gas temperature is higher than 1300°C in Figure 14 and higher than 1400°C in Figure 15. Such a high peak temperature has also been observed in some mass timber compartment fire tests. In the tests by Pope [19], the peak gas temperature at some locations is close to 1400°C . Such a high temperature is due to the relatively large Q_{vent} value for those case studies. In those case studies, Q_{vent} is equal to 12.52 MW, which is higher than those tests in Sect. 4 (4.13 MW for tests by Hevia and McGregor; 8.20 MW for Tests 1–1, 1–4, 1–5 and 1–6 by Su et al.; and 10.32 MW for Tests 1–2 and 1–3 by Su et al.). According to the Equations 2–5, Q_{vent} is a function of opening size and the net calorific value of the fuel. Those case studies assume the majority of the movable fuel load is wood and $H_{c,\text{eff}}$ is 14 MJ/kg (the net calorific value of wood of 17.5 MJ/kg multiplied by a combustion factor of 0.8). Those values are recommended by Eurocode [44]. However, the tests by McGregor has shown that the net calorific value of movable fuel in their tests are only 12.1 MJ/kg [41, 43]. If $H_{c,\text{eff}}$ is equal to 12.1 MJ/kg , the corresponding Q_{vent} is equal to 10.82 MW. Assuming the total fuel load is

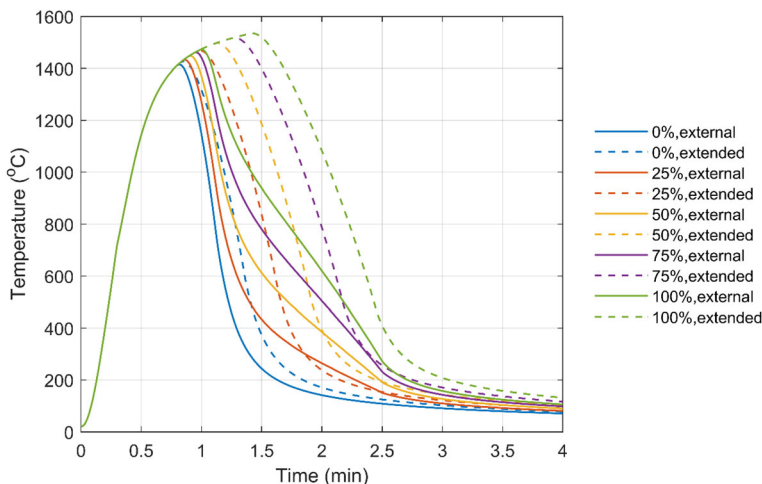


Figure 15. Compartment temperature curves for different amount of exposed surfaces of timber lining (Movable fuel load density is 780 MJ/m^2).

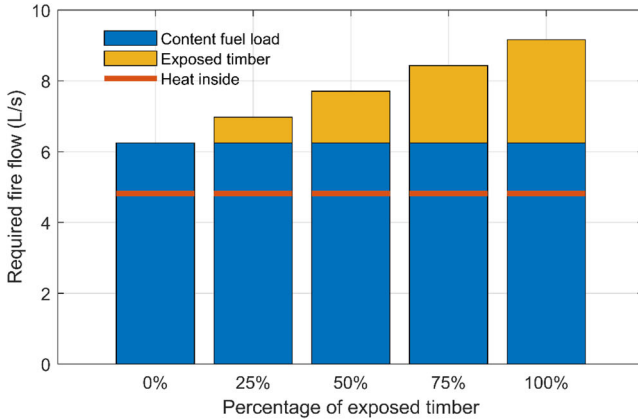
550 MJ/m^2 , the corresponding peak temperature will decrease to 1250°C based on the external flaming combustion model and 1337°C based on the extended fire duration combustion model for the scenario with 100% timber surface exposed.

6.3. Required Water Supply and Fire Flow

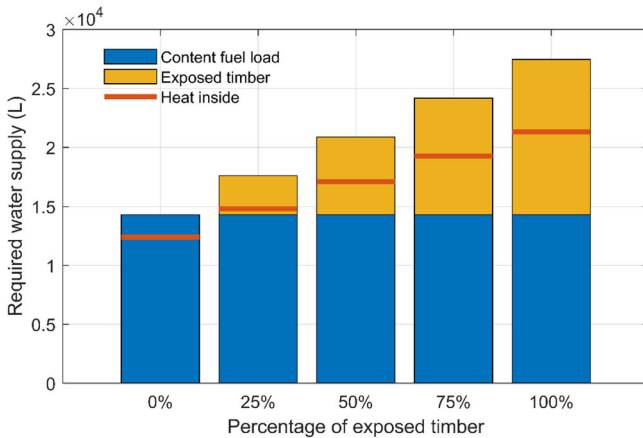
The evaluation of the required firefighting resources to put out a fire in the mass timber building was conducted next. The fire flow and water supply were evaluated using Equations 16 and 18, respectively. It is assumed that the fire is confined in the compartment C1. The movable fuel load is 550 MJ/m^2 . Five percentages of exposed timber are considered, 0% (fully protected), 25%, 50%, 75% and 100% (fully exposed). It is also assumed that CLT panels in this compartment have bond line integrity and encapsulation is in place for the full duration of a fire.

The HRR for the five cases are shown in Figure 13. Here, only the external flaming combustion model is considered. The required fire flow and water supply are evaluated with the method of Sect. 5. The results are plotted in Figure 16. Blue bars represent the contribution of the content fuel load. Yellow bars represent the contribution of the exposed timber. The summation of the two presents the required fire flow or water supply if heat both inside and outside a burning compartment needs to be considered. The values of the orange lines represent the required fire flow or water supply if only the heat inside is considered. F_{inside} was calculated by replacing Q_{max} with Q_{vent} in Equation 15 and S_{inside} was calculated by replacing the energy enclosed by the dash line in Figure 13.

If both heat inside and outside need to be considered, the required fire flow and water supply increase as the exposed timber surface increases. This is because the maximum HRR and the total fuel load contributed by the exposed timber



(a) Fire flow



(b) Water supply

Figure 16. Required fire flow and total water supply for the different scenarios, as a function of the amount of exposed surfaces of timber lining.

increase with the increase of exposed timber surface. As the exposed timber surface increases from 0% to 100%, the required fire flow increases by 47% and the required water supply increases by 91% to balance the additional heat contributed by the burning timber.

If only the heat inside the compartment is considered, the required fire flow does not change because the fire is controlled by ventilation, and having exposed timber does not increase the peak HRR in the compartment. However, the required water supply still increases by 72% as the exposed timber surface increases from 0% to 100%, reflecting the fact that exposed timber will lengthen the fire and add to the total energy released in the compartment.

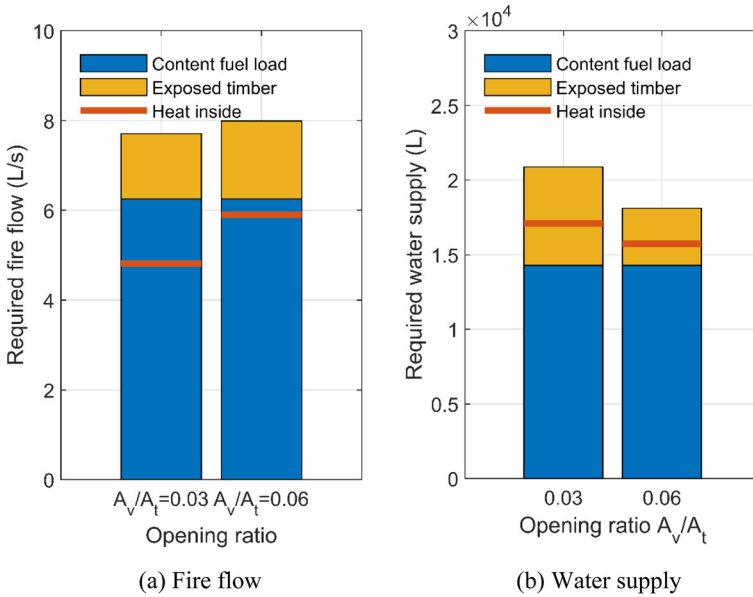


Figure 17. Required fire flow and total water supply as a function of the opening ratio, for compartments with 50% exposed timber surface.

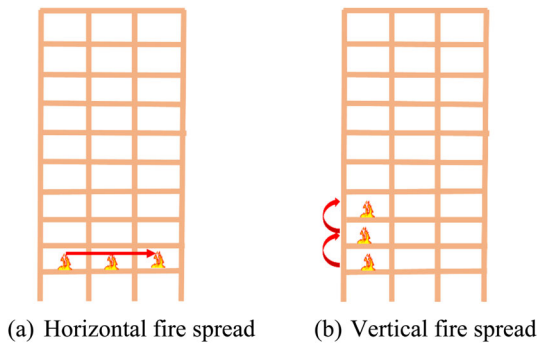


Figure 18. Potential compartmentation failure.

The scenarios plotted in Figure 16 had an opening ratio of $A_v/A_{T1} = 0.03$. In Figure 17, the required fire flow and water supply are evaluated for an opening ratio A_v/A_{T1} of 0.06. The exposed timber surface is 50%. The additional HRR attributable to CLT increases from 0.048 MW/m^2 to 0.060 MW/m^2 , indicating the influence of ventilation on the HRR. If both external and internal firefighting is required, the increase in opening ratios leads to a slight increase in the required fire flow, as shown in Figure 17a. However, the total water supply decreases by 13%, as shown in Figure 17b, because the increase of opening ratio leads to a

decrease in charring depth (e.g., the final charring depth decreases from 46.9 mm to 29.3 mm for the compartment C1), thus a decrease in the total fuel load contributed by the exposed timber surface. If only the internal firefighting is required, the required fire flow is controlled by Q_{vent} that is a function of opening ratio. As the opening ratio increases from 0.03 to 0.06, the required fire flow increases by 22%. In addition, the required water supply decreases by 8%. This reflects the fact that increasing ventilation would lead to a more intense fire (peak HRR increases in the compartment), but of shorter duration.

It should be noted that a compartment fire may spread to adjacent compartments due to the failure of in-story compartmentation (e.g., the failure of the joint connecting CLT wall panels or the burning through of CLT wall panels) or the failure of compartmentation along the height of a building (e.g., fire spreading through external flaming to the upper stories, burning through of CLT floor panels, or failure of the joints connecting CLT floor panels), as shown in Figure 18. Fire spread will increase the demand on the water supply and fire flow dramatically.

7. Conclusion

This study investigated the effect of exposed CLT surfaces in mass timber compartments on the heat release rate, fire severity, and water supply requirements for fire brigades. Existing tall mass timber buildings contain fixed fuel load from timber embedded in the structure. As part of this fixed fuel load may become involved in an uncontrolled fire, it is important to have engineering methods for assessing design fires that account for this contribution. Furthermore, experimental data on compartment fire tests showed that the presence of exposed timber increases the heat release rate and total energy measured, when compared with the same compartments where all timber is protected. The HRR contributed by the exposed CLT may reach the order of 100 kW/m² of exposed CLT over a sustained duration.

A method was presented to evaluate the contribution of exposed timber to the heat release rate in a compartment fire. The method relies on empirical and analytical approaches to assess the ventilation-controlled burning rate and charring depth of the exposed CLT panels. The total HRR is obtained by summing the contributions from the content fuel load and the exposed timber. While the peak HRR in the compartment is limited at any time by the available oxygen, the excess may either be released outside (external flaming combustion model) or at a later time inside the compartment (extended fire duration combustion model). Gas temperature–time relationships can be derived based on these two assumptions to capture the boundaries of possible design fires. In addition, an energy balance method was proposed based on the New Zealand SFPE TP to quantify the water supply required to put out the fires accounting for the contribution of the exposed timber.

A case study of a multi-story mass timber residential building showed application of the proposed methods. The duration and severity of a compartment fire

increased with increasing proportion of exposed CLT surfaces. The potential for heat output outside the compartment, with possible consequences for façade spread and radiation toward neighboring structures, also increased significantly as more of the timber surface was left unprotected. Assuming active fire-safety measures do not work, for a building where the opening ratio is 0.03, 25% of the CLT panel surface is left exposed and the movable fuel load is 550 MJ/m², the duration of heating phase of the fire could increase from 39 min to 46 min. If both internal and external firefighting is required, the required fire flow could increase by up to 12% to balance the additional heat contributed by the burning timber, while the required water supply could increase by up to 23%. If only internal firefighting is required, the required fire flow does not change while the required water supply could increase by up to 19%. These numbers increase further as more of the timber panels are left unprotected. Therefore, this case study illustrates the practical significance of including the contribution of exposed CLT panels when assessing fire scenarios and quantifying thermal exposure conditions. The methods proposed in this paper can be used to incorporate this timber contribution into design fires used in the performance-based fire design of mass timber buildings, with benefits for safety of occupants and fire brigades.

Acknowledgements

This research is based upon work supported by the World Steel Association through grant no. 133408. The views and conclusions contained in this document are those of the authors and should not be interpreted as representing the opinions of the World Steel Association. Mention of trade names or commercial products does not constitute their endorsement by the World Steel Association.

Declarations

Conflict of Interest The authors declare that they have no competing interests.

References

1. Barber D (2018) Fire safety of mass timber buildings with CLT in USA. *Wood Fiber Sci* 50:83–95. <https://doi.org/10.22382/wfs-2018-042>
2. Östman B, Brandon D, Frantzich H (2017) Fire safety engineering in timber buildings. *Fire Saf J* 91:11–20. <https://doi.org/10.1016/j.firesaf.2017.05.002>
3. Buchanan A, Ostman B, Frangi A (2014) White paper on fire resistance of timber structures. Gaithersburg, MD
4. Lange D, Sjöström J, Schmid J et al (2020) A comparison of the conditions in a fire resistance furnace when testing combustible and non-combustible construction. *Fire Technol* 56:1621–1654. <https://doi.org/10.1007/s10694-020-00946-6>
5. Chorlton B, Gales J (2019) Fire performance of cultural heritage and contemporary timbers. *Eng Struct* 201:109739. <https://doi.org/10.1016/j.engstruct.2019.109739>

6. Chorlton B, Gales J (2020) Fire performance of heritage and contemporary timber encapsulation materials. *J Build Eng* 29:101181. <https://doi.org/10.1016/j.jobte.2020.101181>
7. Garcia-Castillo E, Paya-Zaforteza I, Hospitaler A (2021) Analysis of the fire resistance of timber jack arch flooring systems used in historical buildings. *Eng Struct* 243:112679. <https://doi.org/10.1016/j.engstruct.2021.112679>
8. Emberley R, Inghelbrecht A, Yu Z, Torero JL (2017) Self-extinction of timber *Proc Combust Inst* 36:3055–3062. <https://doi.org/10.1016/j.proci.2016.07.077>
9. Bartlett AI (2018) Auto-extinction of engineered timber (dissertation). University of Edinburgh, School of Engineering
10. Su J, Lafrance P-S, Hoehler MS, Bundy MF (2018) Fire safety challenges of tall wood buildings Phase 2: Task 3—cross laminated timber compartment fire tests. Gaithersburg, MD
11. Brandon D (2018) Fire safety challenges of tall wood buildings—Phase 2: Task 4—engineering methods. Boras, Sweden
12. Frangi A, Fontana M, Hugi E, Jübstl R (2009) Experimental analysis of cross-laminated timber panels in fire. *Fire Saf J* 44:1078–1087. <https://doi.org/10.1016/j.fire-saf.2009.07.007>
13. Bartlett AI, McNamee R, Robert F, Bisby LA (2020) Comparative energy analysis from fire resistance tests on combustible versus noncombustible slabs. *Fire Mater* 44:301–310. <https://doi.org/10.1002/fam.2760>
14. Mindeguia J, Mohaine S, Bisby L et al (2021) Thermo-mechanical behaviour of cross-laminated timber slabs under standard and natural fires. *Fire Mater* 45:866–884. <https://doi.org/10.1002/fam.2938>
15. Wiesner F, Bartlett A, Mohaine S et al (2021) Structural capacity of one-way spanning large-scale cross-laminated timber slabs in standard and natural fires. *Fire Technol* 57:291–311. <https://doi.org/10.1007/s10694-020-01003-y>
16. Wiesner F, Bisby LA, Bartlett AI et al (2019) Structural capacity in fire of laminated timber elements in compartments with exposed timber surfaces. *Eng Struct* 179:284–295. <https://doi.org/10.1016/j.engstruct.2018.10.084>
17. Nothard S, Lange D, Hidalgo JP et al (2022) Factors influencing the fire dynamics in open-plan compartments with an exposed timber ceiling. *Fire Saf J* 129:103564. <https://doi.org/10.1016/j.firesaf.2022.103564>
18. Mcnamee R, Zehfuss J, Bartlett AI et al (2020) Enclosure fire dynamics with a cross-laminated timber ceiling. *Fire Mater* . <https://doi.org/10.1002/fam.2904>
19. Pope I, Xu H, Gupta V, et al (2021) Fire dynamics in under-ventilated mass timber room compartments. In: 12th Asia-Oceania Symposium on Fire Science and Technology. The University of Queensland, Brisbane, Australia
20. Bartlett A, Hadden RM, Bisby LA, Law A (2015) Analysis of cross-laminated timber charring rates upon exposure to non-standard heating conditions. In: *Fire and Materials*. San Francisco, USA
21. Bartlett AI, Hadden RM, Bisby LA (2019) A review of factors affecting the burning behaviour of wood for application to tall timber construction. *Fire Technol* 55:1–49. <https://doi.org/10.1007/s10694-018-0787-y>
22. Schmid J, Santomaso A, Brandon D et al (2018) Timber under real fire conditions – the influence of oxygen content and gas velocity on the charring behavior. *J Struct Fire Eng* 9:222–236. <https://doi.org/10.1108/JSFE-01-2017-0013>
23. Richter F, Rein G (2019) Heterogeneous kinetics of timber charring at the microscale. *J Anal Appl Pyrolysis* 138:1–9. <https://doi.org/10.1016/j.jaap.2018.11.019>

24. Mindeguia J, Cueff G, Dréan V, Auguin G (2018) Simulation of charring depth of timber structures when exposed to non-standard fire curves. *J Struct Fire Eng* 9:63–76. <https://doi.org/10.1108/JSFE-01-2017-0011>
25. Richter F, Atreya A, Kotsovinos P, Rein G (2019) The effect of chemical composition on the charring of wood across scales. *Proc Combust Inst* 37:4053–4061. <https://doi.org/10.1016/j.proci.2018.06.080>
26. Gernay T (2021) Fire resistance and burnout resistance of timber columns. *Fire Saf J* 122:103350. <https://doi.org/10.1016/j.firesaf.2021.103350>
27. Crielaard R, Van De KJ, Terwel K et al (2019) Self-extinguishment of cross-laminated timber. *Fire Saf J* 105:244–260. <https://doi.org/10.1016/j.firesaf.2019.01.008>
28. Emberley R, Do T, Yim J, Torero JL (2017) Critical heat flux and mass loss rate for extinction of flaming combustion of timber. *Fire Saf J* 91:252–258. <https://doi.org/10.1016/j.firesaf.2017.03.008>
29. Bartlett AI, Hadden RM, Hidalgo JP et al (2017) Auto-extinction of engineered timber: application to compartment fires with exposed timber surfaces. *Fire Saf J* 91:407–413. <https://doi.org/10.1016/j.firesaf.2017.03.050>
30. Barber D (2017) Determination of fire resistance ratings for glulam connectors within US high rise timber buildings. *Fire Saf J* 91:579–585. <https://doi.org/10.1016/j.firesaf.2017.04.028>
31. Li Z, Luo J, He M et al (2021) Analytical prediction of the fire resistance of the glulam bolted connections under coupled moment and shear. *J Build Eng* 33:101531. <https://doi.org/10.1016/j.jobe.2020.101531>
32. Luo J, He M, Li Z et al (2022) Experimental and numerical investigation into the fire performance of glulam bolted beam-to-column connections under coupled moment and shear force. *J Build Eng* 46:103804. <https://doi.org/10.1016/j.jobe.2021.103804>
33. Shabaniyan M, Braxtan NL (2022) Thermo-mechanical behavior of Glulam beam-to-girder assemblies with steel doweled connections before, during and after fire. *J Struct Fire Eng* . <https://doi.org/10.1108/JSFE-04-2021-0018>
34. Barber D, Avenue C (2015) Tall timber buildings: what 's next in fire. *Fire Technol* 51:1279–1284. <https://doi.org/10.1007/s10694-015-0497-7>
35. Rackauskaite E, Kotsovinos P, Barber D (2021) Letter to the editor : design fires for open-plan buildings with exposed mass-timber. *Fire Technol* 57:487–495. <https://doi.org/10.1007/s10694-020-01047-0>
36. Wade C (2020) Fire design of tall timber buildings. *Build Mag*. 42–43
37. McNamee R, Zehfuss J, Bartlett AI et al (2020) Enclosure fire dynamics with a cross-laminated timber ceiling. *Fire Mater fam* . <https://doi.org/10.1002/fam.2904>
38. Gorska C, Hidalgo JP, Torero JL (2021) Fire dynamics in mass timber compartments. *Fire Saf J* 120:103098. <https://doi.org/10.1016/j.firesaf.2020.103098>
39. Brandon D (2016) Practical method to determine the contribution of structural timber to the rate of heat release and fire temperature of post-flashover compartment fires. SP Technical Research Institute of Sweden, Borås, Sweden
40. Hopkin D, Anastasov S, Brandon D (2017) Reviewing the veracity of a zone-model-based-approach for the assessment of enclosures formed of exposed CLT. In: Martin G, Wang Y (eds) the International Conference of Applications of Structural Fire Engineering (ASFE 2017) CRC Press, Manchester,
41. Wade C, Spearpoint M, Fleischmann C et al (2018) Predicting the fire dynamics of exposed timber surfaces in compartments using a two-zone model. *Fire Technol* 54:893–920. <https://doi.org/10.1007/s10694-018-0714-2>

42. Dixon R (2017) A methodology for quantifying fire resistance level of buildings containing exposed structural timber elements (powerpoint presentation). In: Fire Australia 2017 Conference and Tradeshow. Sydney, Australia
43. McGregor C (2013) Contribution of cross laminated timber panels to room fires (master's thesis). Carleton University
44. EN1991-1-2 (2002) Eurocode 1: actions on structures—Part 1-2: general actions—actions on structures exposed to fire. European Committee for Standardization, Brussels, Belgium
45. Zehfuss J, Hosser D (2007) A parametric natural fire model for the structural fire design of multi-storey buildings. *Fire Saf J* 42:115–126. <https://doi.org/10.1016/j.fire-saf.2006.08.004>
46. Cadorin J, Pintea D, Franssen J (2001) The design fire tool OZone V2.0—theoretical description and validation on experimental fire tests. Belgium
47. EN 1995-1-2. Eurocode 5: Design of timber structures—Part 1-2: General—Structural fire design (2004). European Committee for Standardization
48. Kotsovinos P, Rackauskaite E, Christensen E et al (2022) Fire dynamics inside a large and open-plan compartment with exposed timber ceiling and columns: CodeRed #01. *Fire Mater* . <https://doi.org/10.1002/fam.3049>
49. Crosslam/CLT: performance characteristics (n.d.). In: GreenSpec. <https://www.greenspec.co.uk/building-design/crosslam-timber-performance-characteristics/>. Accessed 19 Feb 2022
50. Canadian Wood Council (2018) Brock Commons, tallwood house, University of British Columbia Vancouver Campus, the advent of tall wood structures in Canada: a case study. Ontario, Canada, Ottawa
51. T3 Minneapolis office building | Mass timber office building (n.d.). In: StructureCraft. <https://structurecraft.com/projects/t3-minneapolis>. Accessed 19 Feb 2022
52. The slow global uprising of cross-laminated timber in construction (2020). In: West Coast Proj. Manag. Inc. <https://www.richardwodehouse.com/the-slow-global-uprising-of-cross-laminated-timber-in-construction/>. Accessed 19 May 2020
53. Wikipedia contributors (2021) Stadthaus. In: Wikipedia, Free Encycl. <https://en.wikipedia.org/w/index.php?title=Stadthaus&oldid=1022724854>. Accessed 19 Feb 2022
54. Aghayere A, Vigil J (2019) Structural wood design: ASD/LRFD, 2nd edn. CRC Press,
55. Structurlam case study Carbon 12, Portland, Oregon (n.d.). In: Structurlam. <https://www.structurlam.com/wp-content/uploads/2017/04/Carbon-12-Case-Study-2.pdf>. Accessed 19 Feb 2022
56. Carbon12 (n.d.). In: Think Wood. <https://www.thinkwood.com/projects/carbon12>. Accessed 19 Feb 2022
57. Abrahamsen R (2018) Mjøstårnet—18 storey timber building completed. In: Internationales Holzbau-Forum IHF 2018. Garmisch-Partenkirchen, Gernay
58. Welc A (2018) Mjøstårnet: World's tallest timber building. In: e-architect. <https://www.e-architect.co.uk/norway/mjoestaarnet-worlds-tallest-timber-building>. Accessed 19 May 2020
59. Mjøstårnet (n.d.). In: Moelven. <https://www.moelven.com/mjostarnet/>. Accessed 19 May 2020
60. Kotecki P (2018) Oregon became first US state to legalize mass timber high-rises. In: Insider. <https://www.businessinsider.com/tall-timber-projects-around-the-world-2018-8>. Accessed 6 Aug 2021
61. Think Wood (n.d.) Design and construction of taller wood buildings. In: Contin. Educ. <https://1r4scx402tmr26fqa93wk6an-wpengine.netdna-ssl.com/wp-content/uploads>

/2020/08/ThinkWood-CEU-Design-and-Construction-of-Taller-Wood-Buildings.pdf.

Accessed 19 Feb 2022

62. Origine (n.d.). In: Think Wood. <https://www.thinkwood.com/projects/origine-tallest-wood-building-in-eastern-north-america>. Accessed 6 Aug 2021
63. World's largest CLT building starts on site in Hackney (2015). In: Constr. Manag. <https://www.constructionmanagermagazine.com/news/worlds-largest-clt-building-starts-site-hackney/>. Accessed 19 May 2020
64. Pitt V (2014) Banyan Wharf: timber tower tops out. In: Building. <https://www.building.co.uk/news/banyan-wharf-timber-tower-tops-out/5072155.article>. Accessed 19 May 2020
65. projects UK CLT (2018). Waugh Thistleton Architects, Canada
66. Treet—a wooden high-rise building with excellent energy performance (n.d.). In: Build Up. <https://www.buildup.eu/en/practices/cases/treet-wooden-high-rise-building-excellent-energy-performance>. Accessed 19 May 2020
67. Griffiths A (2014) Wingårdhs completes prefabricated apartment block built entirely from wood. In: dezeen. <https://www.dezeen.com/2014/07/03/wingardhs-strandparken-wooden-prefabricated-housing-stockholm/>. Accessed 20 May 2020
68. Landel P (2018) Swedish technical benchmarking of tall timber buildings. Borås, Sweden
69. Stora Enso Division Wood Products (2016) Stora Enso CLT: projects. Stockholm, Sweden
70. Two CLT buildings for London's Trafalgar Place, a first for Lendlease in UK (2017). In: Panels Furnit. Asia. [https://www.panelsfurnitureasia.com/en/news-archive/two-clt-buildings-for-london-s-traffic-place-a-first-for-lendlease-in-uk/458#:~:text=Editor's pickTwo CLT buildings, first for Lendlease in UK&text=Trafalgar Place is the flagship,Elephant and Castle in.](https://www.panelsfurnitureasia.com/en/news-archive/two-clt-buildings-for-london-s-traffic-place-a-first-for-lendlease-in-uk/458#:~:text=Editor's%20pickTwo%20CLT%20buildings,%20first%20for%20Lendlease%20in%20UK&text=Trafalgar%20Place%20is%20the%20flagship,Elephant%20and%20Castle%20in.) Accessed 12 Mar 2020
71. Via Cenni (2015). In: Stora Enso. <https://www.storaenso.com/en/newsroom/news/2015/2/via-cenni>. Accessed 6 Aug 2021
72. Cross-laminated timber: the sky's the limit (2012). In: Guard. <https://www.theguardian.com/sustainable-business/cross-laminated-timber-built-environment>. Accessed 6 Aug 2021
73. Kwok A, Zalusky H, Rasmussen L, et al (2019) Cross-laminated timber building: a WBLCA case study series. TALLWOOD Desing Institute
74. Lease L (2013) Forté—building Australia's first timber highrise (Presentation). In: Wood Solutions. Atlanta
75. Castro F (2021) Wood innovation design centre/Michael green architecture. In: Arch-Daily. [https://www.archdaily.com/630264/wood-innovation-design-centre-michael-green-architecture#:~:text=The Wood Innovation Design Centre,for innovative uses of wood.&text=The design incorporates a simple,beams%2C and mass timber walls.](https://www.archdaily.com/630264/wood-innovation-design-centre-michael-green-architecture#:~:text=The%20Wood%20Innovation%20Design%20Centre,for%20innovative%20uses%20of%20wood.&text=The%20design%20incorporates%20a%20simple,beams%2C%20and%20mass%20timber%20walls.) Accessed 6 Aug 2021
76. Wood innovation and design centre (n.d.). In: WSP. <https://www.wsp.com/en-CA/projects/wood-innovation-and-design-centre>. Accessed 6 Aug 2021
77. First timber arrives for the world's largest and tallest engineered timber office building (n.d.). In: Lend Lease Corp. Ltd. <https://www.lendlease.com/-/media/llcom/investor-relations/media-releases/2018/feb/20180215-first-timber-arrives-for-the-worlds-largest-and-tallest-engineered-timber-office-building.ashx>. Accessed 19 Feb 2022
78. King (n.d.). In: Archello. <https://archello.com/project/25-king>. Accessed 6 Aug 2021
79. King, Brisbane, Australia (n.d.). In: Aurecon. <https://www.aurecongroup.com/project/s/property/25-king>. Accessed 6 Aug 2021

80. Ravenscroft T (2017) Dalston Lane: the world's largest timber building. In: BIM. <http://www.theblm.com/video/dalston-lane-the-worlds-largest-timber-building>. Accessed 6 Aug 2021
81. Dalston Lane, London, Great Britain (n.d.). In: binderholz. <https://www.binderholz.com/en/construction-solutions/residential-buildings/dalston-lane-london-great-britain/>. Accessed 6 Aug 2021
82. Esler B (2015) 10 Story all-wood CLT building under construction. In: Woodwork. Netw. <https://www.sbcmag.info/news/2015/aug/10-story-all-wood-clt-building-under-construction>
83. Perkins+Will (2014) Summary report: survey of international tall wood buildings. Forestry Innovation Investment and Binational Softwood Lumber Council
84. Vienna remains different (n.d.). In: Kampmann. <https://www.kampmanngroup.com/Kampmann-Today/Reportages/vienna-remains-different>. Accessed 19 Feb 2022
85. Lightadmin (2018) World's tallest timber building "HoHo Tower" in Vienna. In: Lightwood. <https://lightwood.org/worlds-tallest-timber-building-hoho-tower-in-vienna/>. Accessed 8 Aug 2021
86. Hevia ARM (2014) Fire resistance of partially protected cross-laminated timber rooms (master's thesis). Carleton University
87. Ronquillo G, Hopkin D, Spearpoint M (2021) Review of large-scale fire tests on cross-laminated timber. *J Fire Sci* 39:327–369. <https://doi.org/10.1177/07349041211034460>
88. Richter F, Kotsovinos P, Rackauskaite E, Rein G (2021) Thermal response of timber slabs exposed to travelling fires and traditional design fires. *Fire Technol* 57:393–414. <https://doi.org/10.1007/s10694-020-01000-1>
89. Brandon D, Hopkin D, Emberley R, Wade C (2021) Timber Structures. In: LaMalva K, Hopkin D (eds) *International handbook of structural fire engineering* Springer, Cham, pp 235–322
90. Wiesner F, Hadden R, Deeny S, Bisby L (2022) Structural fire engineering considerations for cross-laminated timber walls. *Constr Build Mater* 323:126605. <https://doi.org/10.1016/j.conbuildmat.2022.126605>
91. Kawagoe K (1958) Fire behaviour in rooms, Report No. 27. Tokyo
92. Schmid J, Frangi A (2021) Structural timber in compartment fires—the timber charring and heat storage model. *Open Eng* 11:435–452. <https://doi.org/10.1515/eng-2021-0043>
93. Insurance Services Offices (2008) *Guide for Determination of Needed Fire Flow*. New Jersey
94. NFPA 1142 (2011) *Water supplies for suburban and rural fire fighting*, 2012nd edn. Quincy, MA
95. Ministry of Municipal Affairs and Housing (2005) *Ontario Building Code 1997*, July 1, 2005 Update. Ontario, Canada
96. National guidance document on the provision of water for fire fighting (2007). Water UK and Local Government Association
97. *International fire code* (2012) 2011. International Code Council, Illinois
98. NFPA 1, *Fire code* (2021) National Fire Protection Association. Quincy, MA
99. Barnett CR (2004) SFPE (NZ) technical publication—TP 2004/1. Calculation methods for water flows used for fire fighting purposes, New Zealand
100. Barnett CR (2005) SFPE (NZ) Technical publication—TP 2005/2. Calculation methods for storage water used for fire fighting purposes, New Zealand

101. EN1991–1–2 (2002) Eurocode 1: actions on structures—Part 1–2: general actions—actions on structures exposed to fire. European Standard, European Committee for Standardization, Belgium
102. Tong Q, Gernay T (2021) A hierarchical Bayesian model for predicting fire ignitions after an earthquake with application to California. *Nat Hazards* . <https://doi.org/10.1007/s11069-021-05109-6>
103. Zelinka SL, Hasburgh LE, Bourne KJ et al (2018) Compartment fire testing of a two-story mass timber building, General Technical Report FPL-GTR-247. Madison, WI
104. Cadorin JF, Pintea D, Dotreppe JC, Franssen JM (2003) A tool to design steel elements submitted to compartment fires—OZone V2. Part 2: methodology and application. *Fire Saf J* 38:429–451. [https://doi.org/10.1016/S0379-7112\(03\)00015-8](https://doi.org/10.1016/S0379-7112(03)00015-8)

Publisher's Note Springer Nature remains neutral with regard to jurisdictional claims in published maps and institutional affiliations.